TNP-AMP Binding to the Sarcoplasmic Reticulum Ca^{2+}-ATPase Studied by Infrared Spectroscopy

Man Liu* and Andreas Barth†
*Institut für Biophysik, Johann Wolfgang Goethe-Universität, Frankfurt am Main, Germany; and †Department of Biochemistry and Biophysics, The Arrhenius Laboratories for Natural Sciences, Stockholm University, Stockholm, Sweden

ABSTRACT Infrared spectroscopy was used to monitor the conformational change of 2′,3′-*O*-(2,4,6-trinitrophenyl)adenosine 5′-monophosphate (TNP-AMP) binding to the sarcoplasmic reticulum Ca^{2+}-ATPase. TNP-AMP binding was observed in a competition experiment: TNP-AMP is initially bound to the ATPase but is then replaced by β,γ-iminoadenosine 5′-triphosphate (AMPPNP) after AMPPNP release from P^3-1-(2-nitrophenyl)ethyl AMPPNP (caged AMPPNP). The resulting infrared difference spectra are compared to those of AMPPNP binding to the free ATPase, to obtain a difference spectrum that reflects solely TNP-AMP binding to the Ca^{2+}-ATPase. TNP-AMP used as an ATP analog in the crystal structure of the sarcoplasmic reticulum Ca^{2+}-ATPase was found to induce a conformational change upon binding to the ATPase. It binds with a binding mode that is different from that of AMPPNP, ATP, and other tri- and diphosphate nucleotides: TNP-AMP binding causes partially opposite and smaller conformational changes compared to ATP or AMPPNP. The conformation of the TNP-AMP ATPase complex is more similar to that of the $E1Ca_2$ state than to that of the $E1ATPCa_2$ state. Regarding the use of infrared spectroscopy as a technique for ligand binding studies, our results show that infrared spectroscopy is able to distinguish different binding modes.

INTRODUCTION

Ca^{2+} transport from the cytoplasm of muscle cells into the sarcoplasmic reticulum (SR), necessary for muscle relaxation, is performed by the SR Ca^{2+}-ATPase (Hasselbach and Makinose, 1961; Hasselbach, 1974; De Meis and Vianna, 1979) which couples ATP hydrolysis to active Ca^{2+} transport. The ATPase undergoes conformational changes upon ATP binding and the subsequent phosphorylation when ATP's γ-phosphate is transferred to *Asp*351. Nucleotide binding to the ATPase has been studied intensively by using fluorescent ATP analogs like trinitrophenyl (TNP) adenosine phosphates (Moczydlowski and Fortes, 1981a), reviewed in McIntosh (1998). TNP-nucleotides have been used not only because of their high fluorescence yield and photolabeling properties, but also on account of their high binding affinity. TNP-ATP, -ADP, and -AMP bind with high affinity to the catalytic sites of the Na^+/K^+-ATPase (Moczydlowski and Fortes, 1981a,b), gastric H^+/K^+-ATPase (Faller, 1989, 1990), and the SR Ca^{2+}-ATPase (Dupont et al., 1982; Dupont and Pougeois, 1983; Watanabe and Inesi, 1982; Berman, 1986; McIntosh et al., 1996). TNP-AMP was used as ATP analog in the crystal structure of the $E1Ca_2$ state of the SR Ca^{2+}-ATPase (Toyoshima et al., 2000). It binds to the catalytic nucleotide binding site of the Ca^{2+}-ATPase (Nakamoto and Inesi, 1984; Suzuki et al., 1990). However, there is evidence that the structure with ATP is different from that with TNP-AMP, since 1), TNP-AMP binding to the ATPase cannot provide strong resistance against proteinase K and V8 whereas ATP and adenosine 5′-(β,γ-methylene)triphosphate (AMPPCP) can (Danko et al., 2001); and 2), ATP binding destroys the $E1Ca_2$ crystals (MacLennan and Green, 2000) in contrast to TNP-AMP (Toyoshima et al., 2000).

Here we investigate the conformational change of TNP-AMP binding to the Ca^{2+}-ATPase in solution by infrared spectroscopy. Conformational changes of the polypeptide backbone upon binding lead to changes in amide I absorption, which is sensitive to secondary structure. The amide I signals therefore provide a fingerprint of the conformational change and enable an estimate of the net change of secondary structure (Barth et al., 1996). In our experiments we trigger nucleotide binding by photolytic release from caged nucleotides to detect the small infrared absorbance changes with high sensitivity (Barth et al., 1990). Unfortunately, a caged derivative of TNP-AMP is not available. Therefore we investigate TNP-AMP binding in an exchange or competition experiment where AMPPNP replaces TNP-AMP from the binding site. AMPPNP is released from caged AMPPNP and this triggers AMPPNP binding in the presence of TNP-AMP. AMPPNP is an excellent model for ATP since it induces very similar conformational changes (Barth et al., 1996; Von Germar et al., 2000; Liu and Barth, 2002) and binds to the same site as ATP (Clore et al., 1982). We use AMPPNP because it is a nonphosphorylating analog of ATP. This prolongs the observation time for the nucleotide ATPase complex compared to ATP and therefore enables a better signal-to-noise ratio of the nucleotide binding spectrum. From the comparison of AMPPNP binding in the presence and absence of TNPAMP we are able to construct a TNPAMP binding spectrum. The results indicate that TNP-AMP induces a conformational change upon binding. The nature of conformational change caused by TNP-AMP binding is different from that caused by ATP or AMPPNP binding. The conformation of the TNP-

Submitted February 3, 2003, and accepted for publication July 25, 2003.
Address reprint requests to Andreas Barth, Tel: 46-816-2452; Fax: 46-815-5597; E-mail: Andreas.Barth@dbb.su.se.

0006-3495/03/11/3262/09 $2.00

AMP ATPase complex is more similar to that of the $E1Ca_2$ state than to that of the $E1ATPCa_2$ state.

MATERIALS AND METHODS

Sample preparation

SR vesicles were prepared as described (De Meis and Hasselbach, 1971). After 60-min dialysis of SR vesicles in 10 mM methylimidazole/HCl, pH 7.5, 0.2 mM $CaCl_2$, and 10 mM KCl, infrared samples were prepared by vacuum drying 15 μL of SR suspension and further additions on a CaF_2 window with a trough of 5-μm depth and 8-mm diameter and resuspending the SR film with ~0.8 μL H_2O. The sample was sealed with a second flat CaF_2 window. The samples contained ~1.2 mM Ca^{2+}-ATPase, 0.5 mg/ml Ca^{2+} ionophore (A23187), 150 mM methylimidazole, 150 mM KCl, 10 mM $CaCl_2$, TNP-AMP, and caged AMPPNP at different concentrations, and DTT at the same concentration as caged AMPPNP.

As a control that the infrared signals are caused by nucleotide binding to the Ca^{2+}-ATPase, thapsigargin (TG) (Kijima et al., 1991; Sagara et al., 1992) was used to selectively inhibit the Ca^{2+}-ATPase in control samples. The control samples were made as described in the following: after 60-min dialysis of SR vesicles in the same buffer but with only 20 μM $CaCl_2$, 15 μL of SR suspension was incubated first with μL of 0.6 mM EGTA for 5 min and then with 1 μL of 1.2 mM TG for 5 min at 20°C. After that the samples were prepared as described in the paragraph above. The concentrations are the same with the exception of the following concentrations in the control samples: 0.3 mM $CaCl_2$, 0.6 mM EGTA, and 1.2 mM TG.

Fourier transform infrared (FTIR) measurements

Time-resolved Fourier transform infrared (FTIR) measurements were performed at 1°C with a modified Bruker (Ettlingen, Germany) IFS 66 spectrometer and recorded with OPUS 3.0 (OS/2 version) at a resolution of 4 cm^{-1} as described previously (Barth et al., 1996). Photolytic release of AMPPNP was triggered by a Xenon flash tube (N-185C, Xenon, Woburn MA), which produces a flash energy (at the area of the sample) of ~150 mJ in the near-ultraviolet spectral range. The concentration of released AMPPNP was determined by the amplitude of the band at 1525 cm^{-1}. A reference spectrum was recorded before the photolysis flash. A spectrum was obtained by averaging time-resolved spectra recorded in the time interval between 3.25 s and 165.4 s after the photolytic release of AMPPNP. From this spectrum the reference spectrum was subtracted to generate the raw difference spectrum.

A normalization of spectra to an identical protein concentration is not necessary to generate the difference spectra, because they are obtained directly from the time-resolved absorbance changes of individual samples. However, when difference spectra of different samples were averaged to improve the signal-to-noise ratio, the difference spectra from different samples were normalized to a identical protein concentration by normalizing the respective absorbance spectra to an amide II absorbance of 0.26 (difference in absorbance between 1546 and 1492 cm^{-1}) as described (Barth and Mäntele, 1998). This prevents the possible predominance of individual samples with high protein content in the averaged difference spectra. The absorbance spectra were recorded before the photolysis flash and AMPPNP binding. The absorbance in the amide II region does not depend on the presence of ATP analogs because the absorbance of ATP and ATP analogs is negligible in this region. The amide II band was chosen because it is less sensitive to errors in water subtraction.

In contrast to difference spectra, normalization is a prerequisite for the generation of the double difference spectrum of TNP-AMP binding, where two normalized difference spectra are subtracted (see below).

Photolysis spectrum

To distinguish ligand-binding signals from signals due to caged AMPPNP photolysis, we prepared control samples where the nucleotide binding sites had already been saturated with AMPPNP at the beginning of the experiment. The composition of these samples was the same as that of samples containing caged AMPPNP and no TNP-AMP, with the exception of 5 mM of added AMPPNP. Photolysis of 10 mM caged AMPPNP in the control samples did not lead to further AMPPNP binding and conformational changes. The spectrum therefore shows only signals caused by the photolysis of caged AMPPNP and is named the *photolysis spectrum*. The conditions of recording the photolysis spectrum are as close as possible to the conditions which were used in our binding and exchange experiments. Ten experiments were averaged for the photolysis spectrum. The photolysis spectrum was interactively subtracted from the raw difference spectra to obtain the *AMPPNP binding spectrum* and the *TNP-AMP → AMPPNP exchange spectrum* (see below). The criterion for the correct multiplication factor for the photolysis spectrum in the subtraction was as described (Von Germar et al., 2000). The subtraction factor was judged to be correct when the 1525 cm^{-1} region of the processed spectrum corresponded to that region in the spectrum obtained with [^{15}N]caged ATP. ^{15}N labeling shifts the band of photolysis at 1525 cm^{-1} to 1499 cm^{-1}, which allows the identification of underlying protein bands at ~1525 cm^{-1}.

AMPPNP binding spectrum

The AMPPNP binding spectrum refers to samples where the released AMPPNP binds to the empty binding site of the ATPase. It was obtained with samples containing caged AMPPNP and no TNP-AMP. Saturation of AMPPNP binding in these experiments was verified by a titration of the AMPPNP binding-induced infrared signals using consecutive releases of AMPPNP from caged AMPPNP. Release of ~3 mM AMPPNP from 10 mM caged AMPPNP in one flash was sufficient to saturate the signals. Spectra of four experiments were averaged with the Bruker spectrometer software OPUS 3.1 (Windows NT version) to obtain the AMPPNP binding spectrum and its standard deviation spectrum (shown in Fig. 4 *B*).

Control spectrum of the control samples

The control spectrum was obtained in the same way as the AMPPNP binding spectrum, using two control samples and applying one flash which released ~3 mM AMPPNP from caged AMPPNP. Photolysis spectrum was subtracted.

TNP-AMP titration of the TNP-AMP → AMPPNP exchange spectra

At the beginning of an exchange experiment, TNP-AMP was bound to the ATPase. After the photolysis flash, ~3 mM AMPPNP were released from 10 mM caged AMPPNP, completed with TNP-AMP, and partially replaced TNP-AMP at the binding sites. The resulting difference spectra are named *TNP-AMP → AMPPNP exchange spectra* or simply the *exchange spectra*. Different concentrations of TNP-AMP were used to determine the TNP-AMP concentration that saturates the binding sites.

AMPPNP titration of the TNP-AMP → AMPPNP exchange spectra

To identify the AMPPNP concentration that nearly completely replaces 5 mM TNP-AMP from the binding sites, we performed an AMPPNP titration of the exchange spectrum in eight consecutive kinetic FTIR experiments on one sample with one flash for each experiment. In these experiments, 5 mM TNP-AMP and 30 mM caged AMPPNP were present. In the first experiment, ~3.7 mM AMPPNP was released; in the second a total of~7 mM AMPPNP was present; and so on (Fig. 3 *C*). Signals from two samples were averaged for the AMPPNP titration of the exchange spectra.

TNP-AMP binding spectrum

The exchange spectrum shows the difference in absorbance between the E1AMPPNPCa$_2$ state and the E1TNP-AMPCa$_2$ state, i.e., absorbance of E1AMPPNPCa$_2$ minus absorbance of E1TNP-AMPCa$_2$. The AMPPNP binding spectrum, measured under the same conditions but without TNP-AMP added, shows the difference in absorbance between the E1AMPPNP-Ca$_2$ state and the E1Ca$_2$ state, i.e., absorbance of E1AMPPNPCa$_2$ minus absorbance of E1Ca$_2$. By subtracting the exchange spectrum from the AMPPNP binding spectrum as shown in Scheme 1, we obtained the difference in absorbance between the E1TNP-AMPCa$_2$ state and the E1Ca$_2$ state, i.e., *the TNP-AMP binding spectrum*: absorbance of E1TNP-AMPCa$_2$ minus absorbance of E1Ca$_2$.

SCHEME 1 Calculation of the TNP-AMP binding spectrum; A(ATPase state) is the infrared absorbance of that state

AMPNP binding spectrum: $\mathbf{A(E1AMPPNPCa_2)\text{-}A(E1Ca_2)}$

minus TNP-AMP → AMPPNP exchange spectrum: $\mathbf{A(E1AMPPNPCa_2)\text{-}A(E1TNP\text{-}AMPCa_2)}$

TNP-AMP binding spectrum: $\mathbf{A(E1AMPPNPCa_2)\text{-}A(E1TNP\text{-}AMPCa_2)}$

Confidence level spectra

As described, the TNP-AMP binding spectrum was obtained by subtracting two normalized difference spectra. To assess the confidence level of a double difference spectrum like this, AMPPNP binding spectra of four samples were divided into two groups with two spectra in each group. The spectra in each group were averaged. The confidence level spectra were obtained by subtracting the averaged spectra. Since three possibilities exist to group the spectra, we obtained three confidence level spectra. These spectra are a check of the reproducibility of the experiments.

Estimation of [E1AMPPNPCa$_2$] from the infrared spectra

The amplitude difference between 1644 and 1627 cm^{-1} in the difference spectrum can be used to estimate the concentration of the AMPPNP-ATPase complex E1AMPPNPCa$_2$, [EA]. At the selected wavenumbers, the spectrum is hardly affected by TNP-AMP binding or dissociation (see *circled positions* in the TNP-AMP binding spectrum in Fig. 4 *A*, which are zero at these wavenumbers) and therefore reflects the concentration of the AMPPNP-ATPase complex. The AMPPNP-induced amplitude difference at a given TNPAMP concentration divided by the maximum amplitude difference at zero TNPAMP concentration gives the ratio between [EA] and the total ATPase concentration [E$_t$] (see Figs. 2 *C* and 3 *C*). This ratio represents the fraction of ATPase that binds AMPPNP, whereas the remaining fraction binds TNP-AMP. Because of the high (mM) concentration of TNP-AMP used here, there is no free ATPase in our samples.

RESULTS

Origin of infrared absorbance changes

Fig. 1 shows the AMPPNP binding spectrum and a control spectrum in which the Ca^{2+}-ATPase was selectively inhibited by thapsigargin in the presence of EGTA (Kijima et al., 1991; Sagara et al., 1992; Fortea et al., 2001). These control samples do not show binding signals. Samples without thapsigargin but with 0.6 mM EGTA showed the AMPPNP binding spectrum with the amplitude reduced to ~50%. This demonstrates that the signals obtained after the release of AMPPNP are induced by AMPPNP binding to the Ca^{2+}-ATPase.

In a previous study (Barth et al., 1991), fluorescein isothiocyanate (FITC) was used to determine the origin of binding signals. FITC labels *Lys*515 of the Ca^{2+}-ATPase and blocks the nucleotide binding site. FITC-labeled samples did not show binding signals either, which indicates that infrared signals are induced by nucleotide binding to the Ca^{2+}-ATPase. Also samples in the presence of 20 mM EGTA alone, where the ATPase was in a Ca^{2+}-free state, did not show significant ATP-induced infrared absorbance changes (Barth et al., 1991). From these control experiments, we infer that our infrared signals were caused by nucleotide binding to the Ca^{2+}-ATPase.

We also investigated whether caged AMPPNP binds to the ATPase. For this we varied the concentrations of caged AMPPNP and ATPase. In the range from 1 mM to 10 mM caged AMPPNP, the binding-induced infrared spectra were identical within experimental errors, but decreased to two-thirds of their amplitude when 30 or 50 mM caged AMPPNP were used. This shows that the conformational change upon AMPPNP binding is unaffected by the concentration of caged AMPPNP up to a concentration of 10 mM. We conclude that caged AMPPNP binds to the ATPase in our samples only when its concentration is >10 mM. This will not be a problem for samples used to study TNP-AMP → AMPPNP exchange. In these samples 30 mM of caged

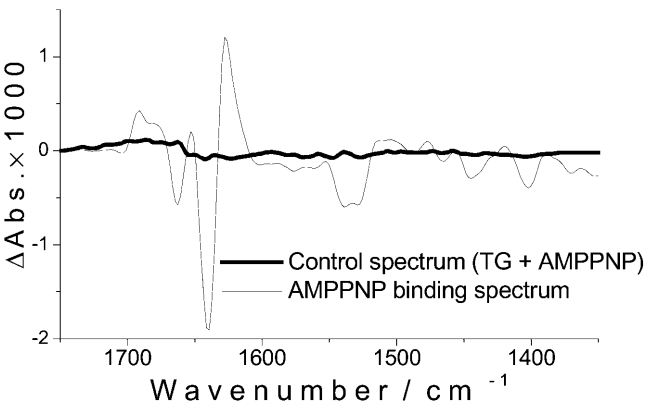

FIGURE 1 Comparison of the AMPPNP binding spectrum and the control spectrum. The AMPPNP binding spectrum (*black thin line*) is the same as in Fig. 2 *B* obtained upon release of 3 mM AMPPNP in SR samples (no TNP-AMP, no TG); the control spectrum (*black bold line*) was obtained upon release of 3 mM AMPPNP in the SR vesicles after incubation with EGTA (0.6 mM) and TG (1.2 mM) as described in Materials and Methods. Absorbance changes due to caged AMPPNP photolysis were subtracted.

AMPPNP was used but the presence of 5 mM TNP-AMP and the high affinity of TNP-AMP ensure that TNP-AMP and not caged AMPPNP is bound to the ATPase initially.

Competition between TNP-AMP and AMPPNP

To perform an experiment where AMPPNP replaces TNP-AMP at the binding site of the Ca^{2+}-ATPase, we first established which concentration of TNP-AMP was needed to saturate the nucleotide binding sites. For this purpose, different concentrations of TNP-AMP were used while the concentration of caged AMPPNP was 10 mM (~3 mM released AMPPNP).

Fig. 2 *A* shows an infrared difference spectrum upon release of 3 mM AMPPNP from caged AMPPNP in the absence of TNP-AMP and the photolysis spectrum that was used for subtraction. It is clear that the subtraction of the photolysis spectrum will not affect either the amplitude or the band positions above 1550 cm^{-1} of the AMPPNP binding spectrum or the TNP-AMP → AMPPNP exchange spectra.

Fig. 2 *B* shows the AMPPNP binding spectrum and TNP-AMP → AMPPNP exchange spectra obtained at different TNP-AMP concentrations. The associated absorption changes cause negative and positive bands in the difference spectra, which are characteristic of the conformation of the enzyme before and after AMPPNP binding, respectively. The difference spectra reflect conformational changes of the protein in the amide I (1700–1610 cm^{-1}) and amide II region (1580–1500 cm^{-1}) of the spectrum. In addition, environmental and structural changes of side chains and nucleotide contribute to the signals in the whole spectral region. As shown in Fig. 2 *B*, increasing the TNP-AMP concentration to 5 mM reduces the amide I signals considerably because TNP-AMP bound to the nucleotide binding site inhibits AMPPNP binding. The positions of the largest bands shift from 1640 and 1627 cm^{-1} in the AMPPNP binding spectrum (no TNP-AMP present) to 1639 and 1626 cm^{-1} in the exchange spectrum, which indicates that AMPPNP replaces TNP-AMP from its binding site (discussed in the subsection called TNP-AMP Binding Spectrum). If AMPPNP bound to empty binding sites, no shift in band position would be expected. No further shift in band position is observed at 10 and 30 mM TNP-AMP. Therefore 5 mM TNP-AMP seem to saturate the nucleotide binding sites under our conditions. At higher TNP-AMP concentrations, the exchange signals decrease further because less TNP-AMP was replaced by AMPPNP from the binding site. This experiment confirms that TNP-AMP and AMPPNP compete for the same binding site on the protein (Bishop et al., 1987; Suzuki et al., 1990), or at least that there is sufficient overlap between the binding sites to ensure efficient competition.

Fig. 2 *C* shows the dependence of the fraction of ATPase bound with AMPPNP on the concentration of TNP-AMP ([EA]/[E_t]; see subsection called Estimation of [E1AMP PNPCa_2] from the Infrared Spectra). The fraction obtained

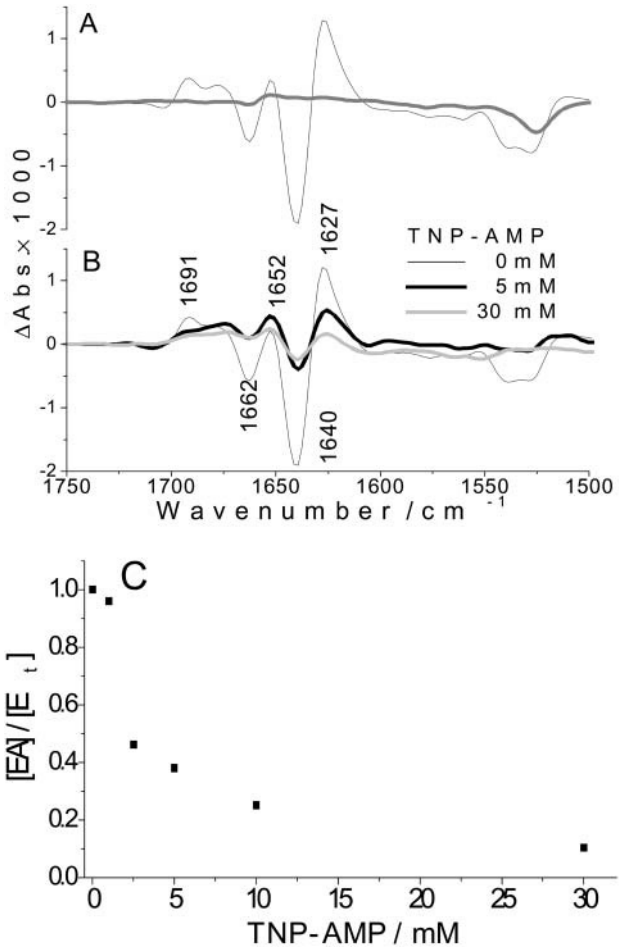

FIGURE 2 Binding of 3 mM AMPPNP to the Ca^{2+}-ATPase in the presence of different TNP-AMP concentrations (1°C, pH 7.5). (*A*) Effects of subtraction of the photolysis spectrum: the raw difference spectrum of 3 mM AMPPNP release in the absence of TNP-AMP without subtraction of the photolysis spectrum and the photolysis spectrum used for subtraction, multiplied by a factor of 0.37. (*B*) The AMPPNP binding spectrum and TNP-AMP → AMPPNP exchange spectra. The labels show the band positions of the AMPPNP binding spectrum (no TNP-AMP). (*C*) Dependence of the fraction of ATPase with bound AMPPNP on the concentration of TNP-AMP, showing the inhibition of AMPPNP binding by TNP-AMP (see subsection called Estimation of [E1AMPPNPCa_2] from the Infrared Spectra). Four experiments were averaged for the AMPPNP binding spectrum in the absence of TNP-AMP. Three and two experiments were averaged for the exchange spectra in the presence of 5 and 30 mM TNP-AMP, respectively.

with 2.5 mM TNP-AMP and 3 mM released AMPPNP is reduced to ~50% at nearly equimolar concentrations, which shows that the affinities of the two nucleotides are similar.

Having identified the TNP-AMP concentration that saturates the binding site, we established the conditions for a nearly 100% exchange of TNP-AMP by AMPPNP in a titration experiment: with a fixed concentration of 5 mM TNP-AMP, we increased the concentration of released AMPPNP with consecutive photolysis flashes (see subsection called AMPPNP Titration of the TNP-AMP →

AMPPNP Exchange Spectrum). Fig. 3 *A* shows the spectrum upon release of ~10 mM AMPPNP in the presence of 5 mM TNP-AMP and the photolysis spectrum that was subtracted to obtain the respective exchange spectrum in Fig. 3 *B* (*thin line*). The small bands at 1664 and 1653 cm^{-1} in the photolysis spectrum may affect the amplitude but not the band positions of the TNP-AMP → AMPPNP exchange spectra in the subtraction of the photolysis spectrum from the raw difference spectrum of the exchange experiment. As shown in Fig. 3 *B*, the signal amplitude of the exchange spectra increase with the increase of released AMPPNP showing that AMPPNP replaces TNP-AMP from the binding sites. In Fig. 3 *C* the fraction of ATPases that bind AMPPNP ([EA] / [E_t]) is plotted against the photolysis band at 1525 cm^{-1}, which is proportional to the concentration of released AMPPNP. The proportion of the AMPPNP-ATPase complex increases until the photolysis band at 1525 cm^{-1} has reached an amplitude of 0.0025 corresponding to ~10 mM released AMPPNP, and shows the plateau from 10 mM of released AMPPNP onwards. Therefore 10 mM of released AMPPNP nearly completely replaces 5 mM TNP-AMP from the binding sites and give saturating TNP-AMP → AMPPNP exchange signals.

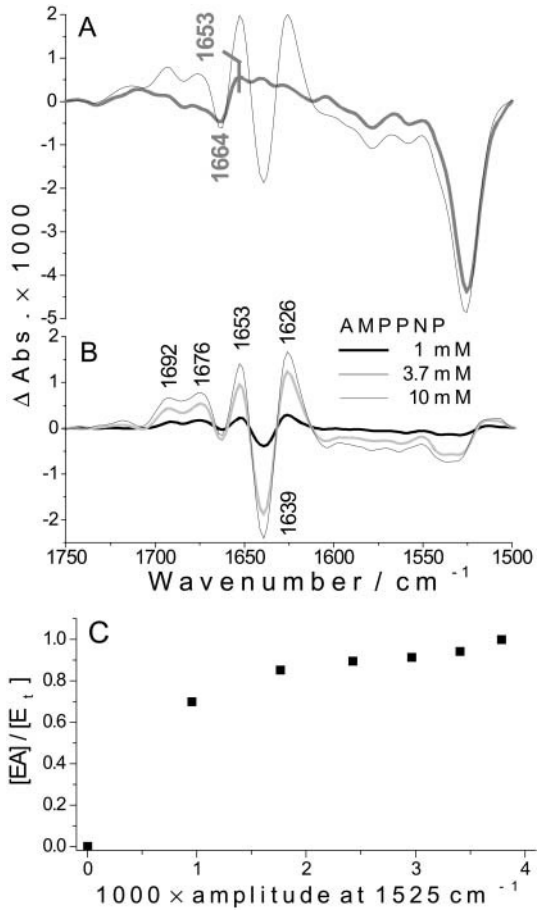

FIGURE 3 TNP-AMP → AMPPNP exchange spectra in the presence of 5 mM TNP-AMP (1°C, pH 7.5). (*A*) Effects of subtraction of the photolysis spectrum: the raw difference spectrum of 10 mM AMPPNP release in the presence of 5 mM TNP-AMP without subtraction of photolysis spectrum and the photolysis spectrum used for the subtraction multiplied by a factor of 1.64. (*B*) TNP-AMP → AMPPNP exchange spectra of the titration with AMPPNP. (*C*) Dependence of the fraction of ATPase with bound AMPPNP on the concentration of released AMPPNP in the presence of 5 mM TNP-AMP (see subsection called Estimation of [E1AMPPNPCa_2] from the Infrared Spectra). Two experiments were averaged for each spectrum or data point.

TNP-AMP binding spectrum

According to Fig. 3 *C*, releasing 10 mM AMPPNP is sufficient to nearly completely substitute 5 mM TNP-AMP in the binding sites of the ATPase. The respective TNP-AMP → AMPPNP exchange spectrum shows similar band positions and band amplitudes as the AMPPNP binding spectrum shown in Fig. 4 *A*. This similarity implies that AMPPNP binding causes similar conformational changes whether or not TNP-AMP is initially bound to the ATPase. However upon closer inspection there are band shifts and amplitude differences between the exchange and the AMPPNP binding spectrum. For example, the bands at 1640 and 1627 cm^{-1} in the AMPPNP binding spectrum shift to 1639 and 1626 cm^{-1} in the exchange spectrum; the amplitude of bands at 1692, 1675, and 1653 cm^{-1} in the exchange spectrum is larger than that of bands at 1692, 1681, and 1652 cm^{-1} in the AMPPNP binding spectrum; and the band at 1607 cm^{-1} is not present in the AMPPNP binding spectrum but is clearly negative in the exchange spectrum.

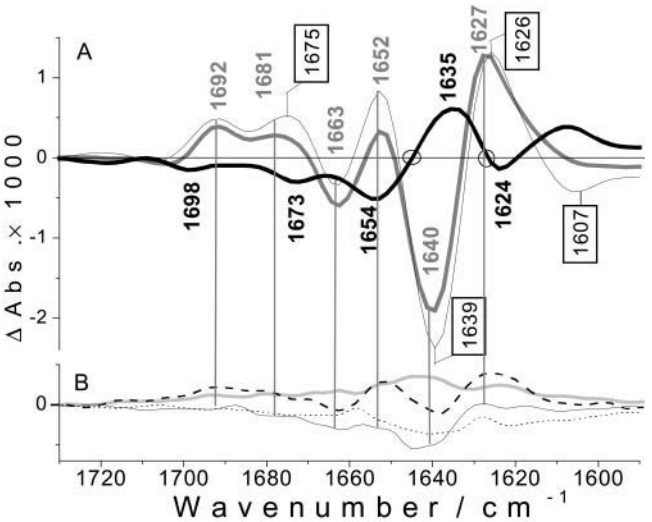

FIGURE 4 (*A*) Comparison of the AMPPNP binding spectrum (*gray line, gray labels*), the TNP-AMP → AMPPNP exchange spectrum at 10 mM released AMPPNP and 5 mM TNP-AMP (*thin line, labels in a box*) and the TNP-AMP binding spectrum (*bold line, bold labels*). (*B*) The standard deviation of AMPPNP binding spectrum (*light gray line*) and three confidence level spectra (for definitions of other lines, see subsections called Confidence Level Spectra, and TNP-AMP Binding Spectrum).

The difference between the respective experiments is that TNP-AMP dissociation from the binding site contributes to the exchange spectrum but not to the AMPPNP binding spectrum where AMPPNP binds to the empty site. The spectral differences between the spectra indicate that TNP-AMP dissociation from the binding site causes conformational changes in addition to those of AMPPNP binding.

By subtracting the exchange spectrum from the AMPPNP binding spectrum, the TNP-AMP binding spectrum (*bold line* in Fig. 4 *A*) is obtained (see subsection called TNP-AMP Binding Spectrum; see also Scheme 1), which shows the infrared absorbance changes associated with TNP-AMP binding. This spectrum is very different from the AMPPNP binding spectrum or the ATP binding spectrum (Barth et al., 1996; Von Germar et al., 2000; Liu and Barth, 2002), with smaller bands often of opposite sign and at slightly different positions. This indicates that TNP-AMP binding induces different and minor conformational changes compared to AMPPNP binding.

The TNP-AMP binding spectrum was obtained in a less direct way than the AMPPNP binding spectrum and the exchange spectrum, since it is the subtraction between two normalized difference spectra. Therefore we discuss below the significance of bands in the TNP-AMP binding spectrum by assessing the variations of band amplitudes and band positions between different samples. Fig. 4 *B* shows the standard deviation of the AMPPNP binding spectrum and the confidence level spectra to the same scale as in Fig. 4 *A*. Confidence level spectra assess the significance of bands in a double difference spectrum. They were calculated from the four AMPPNP binding spectra obtained with four samples as described in the subsection called AMPPNP Binding Spectrum. In these confidence level spectra, small bands at 1663, 1652, 1640, and 1627 cm^{-1} were observed. These bands are caused by small deviations in band amplitude between the individual experiments. Therefore the largest bands in the confidence level spectra are usually observed at peak positions of the AMPPNP binding spectrum. Bands of the TNP-AMP binding spectrum are generally larger than those of the confidence spectra in the same spectral region and all bands labeled in bold in Fig. 4 *A* were also observed in additional experiments in which the released AMPPNP was not enough to saturate the amplitude of the exchange spectrum (data not shown). Despite that, we are careful to attribute the small bands above 1680 cm^{-1} to a conformational change upon TNP-AMP binding inasmuch as it is difficult to prove this rigorously. However, it is evident that the bands at 1635 and 1624 cm^{-1} in the TNP-AMP binding spectrum show real differences between the TNP-AMP → AMPPNP exchange spectrum and the AMPPNP binding spectrum. These bands cannot be explained by a different band amplitude in the difference spectra used in the subtraction. Instead their effect can be detected already upon comparing the AMPPNP binding and the exchange spectrum, where they lead to different band positions: peak positions vary for the AMPPNP binding spectra of the four individual experiments from 1626.9 to 1627.3 cm^{-1} and from 1639.9 to 1640.4 cm^{-1} and for the exchange spectra of two individual experiments from 1639.2 to 1639.3 cm^{-1}. At 1625.9 cm^{-1} the latter show the same peak position for both experiments. The two peak positions are therefore clearly different in the AMPPNP binding spectrum and the TNPAMP → AMPPNP exchange spectrum. Also the 1654 cm^{-1} band of the TNP-AMP binding spectrum is observed at a position different from that in either the AMPPNP binding spectrum or the exchange spectrum, and the band at 1673 cm^{-1} leads to a clearly different shape in the AMPPNP binding spectrum and the exchange spectrum. Subtraction of the photolysis spectrum hardly affects peak positions since it changes the peak position only in one case by 0.1 cm^{-1}. Therefore the different band positions in the AMPPNP and the exchange spectrum are a clear indication of spectral differences.

DISCUSSION

We have chosen TNP-AMP for our infrared study because it was the nucleotide for which binding could be observed in the ATPase crystals. The structure of the ATPase with bound Ca^{2+} and TNP-AMP is not significantly different from that in the absence of TNP-AMP (Toyoshima et al., 2000; Lee and East, 2001), whereas ATP binding to the ATPase causes a conformational change that destroys the crystals. In solution, we detect a conformational change upon binding of TNP-AMP to the SR Ca^{2+}-ATPase which is smaller than that induced by binding of ATP or AMPPNP. Therefore, infrared spectroscopy has detected a difference in the structures of $E1Ca_2$ and $E1TNP\text{-}AMPCa_2$ that was not detected by x-ray crystallography (Toyoshima et al., 2000).

The bands in the amide I region of the TNP-AMP binding spectrum indicate that several secondary structure elements are involved in TNP-AMP binding to the ATPase. Structure changes of β-sheets can induce the bands at 1635 and 1624 cm^{-1}, of α-helices at 1654 cm^{-1}, and of turns at 1673 cm^{-1}. In line with this, several residues of the ATPase in different secondary structures have been found to be involved in TNP-AMP binding: *Thr*441 in an α-helix is close to the surface of the nucleotide binding site and interacts with the TNP moiety (Toyoshima et al., 2000; Abu-Abed et al., 2002). *Lys*515 in a β-strand, and *Phe*487 and *Arg*560 in loops interact with the adenine moiety (McIntosh, 2000; Toyoshima et al., 2000; Abu-Abed et al., 2002).

In another line of studies, we propose that the conformational changes caused by nucleotide binding are characteristic of the bound nucleotides and several functional groups of ATP have been found to be important for the binding-induced conformational change such as the γ-phosphate group (Liu and Barth, 2002), the 2′- and 3′-OH groups in the ribose ring, and the 6-membered ring of adenine (Liu and Barth, 2003). The most likely explanation for this is a direct

interaction of these groups with the protein. The binding mode for the ATP analogs investigated (ITP, 2′-, and 3′-deoxyATP, ADP) seems, however, to be similar to that of ATP, since the shape of the spectra in the amide I region is similar: they all show bands of the same sign as ATP or AMPPNP near 1627, 1640, and 1652 cm^{-1}, and so do most of them near 1662 and 1691 cm^{-1}. Table 1 compares the positions of bands and shoulders for these close ATP derivatives (Liu and Barth, 2003) with those of TNP-AMP (this work). It can be seen that the character of the conformational change caused by TNP-AMP binding is largely opposite to that induced by the other nucleotides: positive bands in the spectra of close ATP derivatives (near 1680, 1652, and 1628 cm^{-1}) appear as negative bands at similar positions in the TNP-AMP binding spectrum (at 1673, 1654, and 1624 cm^{-1}); a negative band (near 1640 cm^{-1}) is positive at similar position in the TNP-AMP binding spectrum (at 1635 cm^{-1}). The opposite character of the TNP-AMP binding-induced spectrum is particularly striking in the region of the largest bands, below 1660 cm^{-1}, where all TNP-AMP bands have a sign opposite to that of all bands of the other nucleotides investigated. If the conformational change upon binding is described by a one-dimensional parameter, similar to a reaction coordinate, then the ATPase complexes with TNP-AMP and ATP lie on opposite ends of the scale with the nucleotide free state $E1Ca_2$ in between, but closer to the TNP-AMP complex.

We think that the particular binding mode observed for TNP-AMP is most likely due to the bulky TNP group attached to the ribose moiety. This is because removal of single functional groups of ATP (2′-OH, 3′-OH, or γ-phosphate) leads mainly to a reduction in band amplitude compared to the ATP binding spectrum but retains most of the spectral shape (Liu and Barth, 2003). From this we infer that binding of the nucleotide moiety of TNP-AMP on its own to the ATPase would lead to a further reduction in band amplitude since it lacks three functional groups that are important for the conformational change of the Ca^{2+}-ATPase: the 2′-OH, the 3′-OH, and the γ-phosphate group; and, in addition, lacks the β-phosphate, which is important for affinity (Lacapere et al., 1990). This will make the nucleotide moiety of TNP-AMP a low affinity ligand for the Ca^{2+}-ATPase. Therefore we attribute the high affinity of TNP-AMP and its particular binding mode detected here to the TNP moiety of TNP-AMP.

The extent of conformational change can be estimated by calculating the index of the change of backbone structure and interaction (COBSI, see Barth et al., 1996). This index is sensitive to secondary structure changes, changes in hydrogen bonding to peptide groups, and subtle structural changes within a given secondary structure. Only net changes are revealed. The index of COBSI with ATP binding is 7.5×10^{-4}, and the index of COBSI with AMPPNP and TNP-AMP binding is 7.0×10^{-4} and 3.1×10^{-4}, respectively. This shows that the extent of conformational changes induced by TNP-AMP binding is significant, being one-third to one-half that of ATP and AMPPNP.

In our previous article (Liu and Barth, 2003) we discussed that infrared spectroscopy will detect indirectly the anticipated hinge movement between nucleotide binding domain N and phosphorylation domain P (Danko et al., 2001). This hinge domain is thought to close the cleft between N and P domain. Since the conformational changes upon TNP-AMP binding have an opposite character to those of ATP binding, we propose as a working hypothesis that TNP-AMP binding opens the cleft. In line with that assumption, the cleft is wide open in the crystal structure of $E1TNP\text{-}AMPCa_2$ (Toyoshima et al., 2000).

The TNP-AMP binding spectrum is somewhat similar to the ADP-binding spectrum of mitochondrial creatine kinase induced by caged ADP photolysis with negative bands at 1651 and 1624 cm^{-1} and a positive band at 1640 cm^{-1} (Raimbault et al., 1996) which indicates a similar binding mode.

From a methodological point of view, we demonstrate that competition experiments can be performed in the infrared spectral region, from which relative dissociation constants can be obtained without the need to develop a binding assay,

TABLE 1 Position of bands and shoulders in the nucleotide binding spectra in the amide I region

Nucleotide	ATP	AMPPNP	ADP	2′-dATP	3′-dATP	ITP	TNP-AMP
Band positions							1698(−)
	1693(+)	1692(+)	1693(+)	1693(+)	1692(+)	1691(+)	
	1680(+)	1681(+)	1680(+, *s*)	1682(+)		1679(+)	
		1678(+, *s*)					
	1673(−, *s*)			1671(−, *s*)	1672(−, *s*)		1673(−)
	1664(−)	1663(−)	1663(−)	1665(−)	1664(−, *s*)	1663(−)	
	1652(+)	1652(+)	1652(+)	1652(+)	1653(+)	1652(+)	**1654(−)**
	1641(−)	1640(−)	1641(−)	1641(−)	1642(−)	1641(−)	**1635(+)**
	1628(+)	1627(+)	1628(+)	1628(+)	1628(+)	1626(+)	**1624(−)**
			1616(+, *s*)	1616(+, *s*)	1616(+, *s*)		
							1607(+)

Key: *s*, shoulder; +, positive band or shoulder; and −, negative band or shoulder. TNP-AMP bands with a sign opposite to ATP-binding binds are indicated in bold.

and confirm that different binding modes of ligands can be detected as shown before (White and Wharton, 1990; Murray et al., 1994; Ryan and Baenziger, 1999; and reviewed in Wharton, 2000). Applications like this will soon gain importance in fundamental and applied research when mixing devices become commercially available that makes these experiments just as easy to perform in the infrared spectral region as in the visible spectral range. The advantage of infrared spectroscopy as a marker-free technique that directly observes protein and ligand can then fully be exploited.

This work was supported by DFG grant Ba1887/2-1. The authors thank W. Mäntele (Johann Wolfgang Goethe-Universität, Frankfurt am Main) for continuous support and provision of facilities, W. Hasselbach (Max-Planck-Institut, Heidelberg) for the gift of the Ca^{2+}-ATPase, J. E. T. Corrie (National Institute for Medical Research, London), and F. von Germar for helping with the preparation of caged compounds.

REFERENCES

Abu-Abed, M., T.-K. Mal, M. Kainosho, D.-H. Maclennan, and M. Ikura. 2002. Characterization of the ATP-binding domain of the sarco(endo)-plasmic reticulum Ca^{2+}-ATPase: probing nucleotide binding by multidimensional NMR. *Biochemistry*. 41:1156–1164.

Barth, A., W. Mäntele, and W. Kreutz. 1990. Molecular changes in the sarcoplasmic reticulum Ca^{2+}-ATPase during catalytic activity. A Fourier transform infrared (FTIR) study using photolysis of caged ATP to trigger the reaction cycle. *FEBS Lett*. 277:147–150.

Barth, A., W. Mäntele, and W. Kreutz. 1991. Infrared spectroscopic signals arising from ligand binding and conformational changes in the catalytic cycle of sarcoplasmic reticulum Ca^{2+} ATPase. *Biochim. Biophys. Acta*. 1057:115–123.

Barth, A., F. von Germar, W. Kreutz, and W. Mäntele. 1996. Time-resolved infrared spectroscopy of the Ca^{2+} ATPase. The enzyme at work. *J. Biol. Chem*. 271:30637–30646.

Barth, A., and W. Mäntele. 1998. ATP-induced phosphorylation of the sarcoplasmic reticulum Ca^{2+} ATPase-molecular interpretation of infrared difference spectra. *Biophys. J*. 75:538–544.

Berman, M. C. 1986. Absorbance and fluorescence properties of 2′(3′)-*O*-(2,4,6-trinitrophenyl)adenosine 5′-triphosphate bound to coupled and uncoupled Ca^{2+}-ATPase of skeletal muscle sarcoplasmic reticulum. *J. Biol. Chem*. 261:16494–16501.

Bishop, J. E., M. K. Al-Shawi, and G. Inesi. 1987. Relationship of the regulatory nucleotide site to the catalytic site of the sarcoplasmic reticulum Ca^{2+}-ATPase. *J. Biol. Chem*. 262:4658–4663.

Clore, G. M., A. M. Gronenborn, C. Mitchinson, and N. M. Green. 1982. ^{1}H-NMR studies on nucleotide binding to the sarcoplasmic reticulum Ca^{2+} ATPase. *Eur. J. Biochem*. 128:113–117.

Danko, S., K. Yamasaki, T. Daiho, H. Suzuki, and C. Toyoshima. 2001. Organization of cytoplasmic domains of sarcoplasmic reticulum Ca^{2+}-ATPase in E_1P and E_1ATP states: a limited proteolysis study. *FEBS Lett*. 505:129–135.

De Meis, L., and W. Hasselbach. 1971. Acetyl phosphate as substrate for calcium uptake in skeletal muscle microsomes. *J. Biol. Chem*. 246:4759–4763.

De Meis, L., and A. Vianna. 1979. Energy interconversion by the Ca^{2+}-dependent ATPase of the sarcoplasmic reticulum. *Annu. Rev. Biochem*. 48:275–292.

Dupont, Y., Y. Chapron, and R. Pougeois. 1982. Titration of the nucleotide binding sites of sarcoplasmic reticulum Ca^{2+}-ATPase with 2′,3′-*O*-(2,4,6-trinitrophenyl) adenosine 5′-triphosphate and 5′-diphosphate. *Biochem. Biophys. Res. Commun*. 106:1272–1279.

Dupont, Y., and R. Pougeois. 1983. Evaluation of H_2O activity in the free or phosphorylated catalytic site of Ca^{2+}-ATPase. *FEBS Lett*. 156:93–98.

Faller, L. D. 1989. Competitive binding of ATP and the fluorescent substrate analogue 2′,3′-*O*-(2,4,6-trinitrophenyl-cyclohexadienylidine)a-denosine 5′-triphosphate to the gastric H^+,K^+-ATPase: evidence for two classes of nucleotide sites. *Biochemistry*. 28:6771–6778.

Faller, L. D. 1990. Binding of the fluorescent substrate analogue 2′,3′-*O*-(2,4,6-trinitrophenylcyclohexadienylidene)adenosine 5′-triphosphate to the gastric H^+,K^+-ATPase: evidence for cofactor-induced conformational changes in the enzyme. *Biochemistry*. 29:3179–3186.

Fortea, M. I., F. Soler, and F. Fernandez-Belda. 2001. Unravelling the interaction of thapsigargin with the conformational states of Ca^{2+}-ATPase from skeletal sarcoplasmic reticulum. *J. Biol. Chem*. 276:37266–37272.

Hasselbach, W. 1974. Sarcoplasmic Reticulum ATPases. *In* The Enzymes, 3rd Ed. P. D. Boyer, editor. Academic Press, New York, London. 431–467.

Hasselbach, W., and M. Makinose. 1961. Die calciumpumpe der ''Erschlaffungsgrana'' des muskels und ihre abhängigkeit von der atp-spaltung. *Biochem. Z*. 333:518–528.

Kijima, Y., E. Ogunbunmi, and S. Fleischer. 1991. Drug action of thapsigargin on the Ca^{2+} pump protein of sarcoplasmic reticulum. *J. Biol. Chem*. 266:22912–22918.

Lacapere, J.-J., N. Bennett, Y. Dupont, and F. Guillain. 1990. pH and magnesium dependence of ATP binding to SR ATPase. *J. Biol. Chem*. 265:348–353.

Lee, A., and J. East. 2001. What the structure of a calcium pump tells us about its mechanism. *Biochem. J*. 356:665–683.

Liu, M., and A. Barth. 2002. Mapping nucleotide binding site of calcium ATPase with IR spectroscopy: effects of ATP gamma-phosphate binding. *Biospectroscopy*. 67:267–270.

Liu, M., and A. Barth. 2003. Mapping interactions between the Ca^{2+}-ATPase and its substrate ATP with infrared spectroscopy. *J. Biol. Chem*. 278:10112–10118.

MacLennan, D. H., and N. M. Green. 2000. Pumping ions. *Nature*. 405: 633–634.

McIntosh, D. B. 1998. The ATP binding sites of P-type ion transport ATPase: properties, structure, conformations, and mechanism of energy coupling. *Adv. Mol. Cell Biol*. 23A:33–99.

McIntosh, D. B. 2000. Portrait of a P-type pump. *Nat. Struct. Biol*. 7: 532–535.

McIntosh, D. B., D. G. Woolley, B. Vilsen, and J. P. Andersen. 1996. Mutagenesis of segment ^{487}Phe-Ser-Arg-Asp-Arg-Lys^{492} of sarcoplasmic reticulum Ca^{2+}-ATPase produces pumps defective in ATP binding. *J. Biol. Chem*. 271:25778–25789.

Moczydlowski, E. G., and P. A. G. Fortes. 1981a. Characterization of 2′,3′-*O*-(2,4,6-trinitrocyclohexadienylidine)adenosine 5′-triphosphate as a fluorescent probe of the ATP site of sodium and potassium transport adenosine triphosphatase. *J. Biol. Chem*. 256:2346–2356.

Moczydlowski, E. G., and P. A. G. Fortes. 1981b. Inhibition of sodium and potassium adenosine triphosphatase by 2′,3′-*O*-(2,4,6-trinitrocyclohex-adienylidene) adenine nucleotides. *J. Biol. Chem*. 256:2357–2366.

Murray, I. A., J. P. Derrick, A. J. White, K. Drabble, C. W. Wharton, and W. V. Shaw. 1994. Analysis of hydrogen bonding in enzyme-substrate complexes of chloramphenicol acetyltransferase by infrared spectroscopy and site-directed mutagenesis. *Biochemistry*. 33:9826–9830.

Nakamoto, R. K., and G. Inesi. 1984. Studies of the interactions of 2′,3′-*O*-(2,4,6-trinitrocyclohexyldienylidine)adenosine nucleotides with the SR (Ca^{2+} + Mg^{2+})-ATPase active site. *J. Biol. Chem*. 259:2961–2970.

Raimbault, C., R. Buchet, and C. Vial. 1996. Changes of creatine kinase secondary structure induced by the release of nucleotides from caged compounds—an infrared difference-spectroscopy study. *Eur. J. Biochem*. 240:134–142.

Ryan, S. E., and J. E. Baenziger. 1999. A structure-based approach to nicotinic receptor pharmacology. *Mol. Pharmacol*. 55:348–355.

Sagara, Y., F. Fernandez-Belda, L. De Meis, and G. Inesi. 1992. Characterization of the inhibition of intracellular Ca^{2+} transport ATPases by thapsigargin. *J. Biol. Chem*. 267:12606–12613.

Suzuki, H., T. Kubota, K. Kubo, and T. Kanazawa. 1990. Existence of a low-affinity ATP-binding site in the unphosphorylated Ca^{2+}-ATPase of sarcoplasmic reticulum vesicles: evidence from binding of 2′,3′-*O*-(2,4,6-trinitrocyclohexadienylidene)-[^{3}H]AMP and -[^{3}H]ATP. *Biochemistry*. 29:7040–7045.

Toyoshima, C., M. Nakasako, H. Nomura, and H. Ogawa. 2000. Crystal structure of the calcium pump of sarcoplasmic reticulum at 2.6 Å resolution. *Nature*. 405:647–655.

Von Germar, F., A. Barth, and W. Mäntele. 2000. Structural changes of the sarcoplasmic reticulum Ca^{2+} ATPase upon nucleotide binding studied by Fourier transform infrared spectroscopy. *Biophys. J*. 78:1531–1540.

Watanabe, T., and G. Inesi. 1982. The use of 2′,3′-*O*-(2,4,6-trinitrophenyl)adenosine 5′-triphosphate for studies of nucleotide interaction with sarcoplasmic reticulum vesicles. *J. Biol. Chem.* 257:11510–11516.

Wharton, C. W. 2000. Infrared spectroscopy of enzyme reaction intermediates. *Nat. Prod. Rep*. 17:447–453.

White, A. J., and C. W. Wharton. 1990. Hydrogen-bonding in enzyme catalysis. Fourier-transform infrared detection of ground-state electronic strain in acyl-chymotrypsins and analysis of the kinetic consequences. *Biochem. J*. 270:627–637.